Organic Photosensor in Elgraphy (II): Photoinduced Current Amplifying Layer

D. Aoki,▲ M. Kashiwabara, M. Okabe, S. Hikosaka, and E. Inoue▲

Central Research Institute Dainippon Printing Co., Ltd., Chiba-Ken, Japan

The authors are actively involved in the development of Elgraphy: a novel image acquiring system that combines electrophotography and liquid crystal technology. The organic photosensor used in Elgraphy (Elgraphic photosensor) exhibits enhanced hole injection induced by a negative space charge trapped at the electrode/photoconductive layer interface, thus giving rise to photocurrent amplification. A new type of photosensor that contains a PICAL (Photoinduced Current Amplifying Layer) between the transparent electrode and the CGL was fabricated. This three layer sensor was found to exhibit significantly larger photocurrent amplification than two layer sensors, that is, the dark current was smaller and the photocurrent was larger in the steady state when the proper voltage was applied. An investigation into how the resistivity of the PICAL and CGL affect the dark current and photocurrent of the three layer photosensor revealed the mechanism involved. The transient variation in the electric field across the PICAL promotes the injection of holes from the electrode, thus enhancing photocurrent amplification. In areas of the sensor that are not exposed to light, the larger resistance of the CGL reduces the voltage across the PICAL, suppressing hole injection from the electrode. In contrast, in areas that are exposed to light, the resistance of the CGL is smaller and the voltage across the PICAL is larger, thus enhancing hole injection.

Journal of Imaging Science and Technology 44: 179–187 (2000)

Introduction

The authors are engaged in the development of Elgraphy:[1–3] a novel high resolution, high sensitivity image acquiring system using dry processes. The intermediate medium for image strage in Elgraphy is made of a layer of organic photosensor and liquid crystal polymer composite layers. The Elgraphic photosensor has a two layer configuration consisting of a CGL (Charge Generation Layer) and a CTL (Charge Transport Layer) formed on the surface of a transparent electrode. The space charge trapped at the electrode/CGL interface induces hole injection from the electrode, thus giving rise to photocurrent amplification.[4,5]

This article reports the findings of our investigation of a new type of Elgraphic photosensor made by inserting a photoinduced current amplifying layer (PICAL) containing an electron acceptor material between the electrode and the CGL. This three layer design enables the electron trapping mechanism to be isolated from the electron generation and electron transport mechanisms. The new photosensor exhibits significantly more efficient photocurrent amplification than two layer photosensors, and also allows a wider range of materials to be used for the CGM and CTM. Investigations into the effects of the PICAL revealed a different amplification mechanism from that of two layer photosensors.

Original manuscript received November 19, 1998

▲ IS&T Member

Experiment

Configuration of Photosensors

Figure 1 shows the configuration of Elgraphic photosensors. Two photoconductive layers, an organic charge generation layer (CGL), followed by a charge transport layer (CTL), are stacked on a transparent electrode formed on a glass substrate. The CGL generates photocarriers and the CTL transports them. Another type of sensor was fabricated that had an additional layer between the electrode and the CGL called the photoinduced current amplifying layer (PICAL). It is intended to trap electrons generated thermally or by incident photons and thus provide control over hole injection from the electrode.

Formation of PICAL

The PICAL was made in the following way. The bisazo pigment material (Dainichiseika Color & Chemicals MFG. Co., Ltd., Japan), shown below, dispersed in polyvinylformal resin (PVF) (3:1 by weight). The mixture was dissolved in an organic solvent, such as cyclohexane

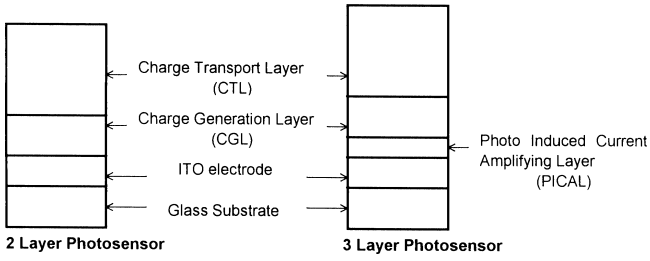

Figure 1. Structure of photosensors.

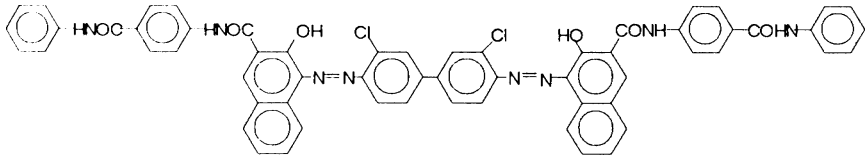

Bis-Azo Pigment

TABLE I. Electron Acceptors and Their Electron Affinities

	Acceptors	Electron Affinity (eV)
A1	1,3-dinitrobenzene	0.30
A2	p-benzoquinone	0.77
A3	2,4,7-trinitrofluorenone	1.10
A4	2,5-dichloro-p-benzoquinone	1.15
A5	2,4,5,7-tetranitrofluorenone	1.21
A6	p-chloranil	1.37
A7	o-chloranil	1.55
A8	7,7,8,8,-tetracyanoquinodimehtane	1.70
A9	2,3-dichloro-5,6-dicyano-p-benzoquinone	1.95

or dioxane (2 to 3 wt%), and dispersed by using a paint shaker or a ball mill.

Resin coatings were made by adding 2 to 8% by weight of the electron acceptor materials shown in Table I to this mixture of bis-azo pigment and binder. The resin mixture was then spin coated on an ITO substrate and dried at 100°C for 20 min in a clean oven. The final thickness was 0.1 to 0.3 μm.

Formation of Charge Generation Layer (CGL)

CGL formed by chemical vapor deposition (CVD) was also made by evaporating thiopyrolopyrrole pigment (DTPP) (shown below) at a rate of 20 A/sec in a vacuum of 5×10^{-6} Torr. The film was left in an acetone vapor atmosphere for an hour.

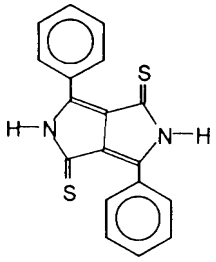

Thiopyrolopyrrole pigment (DTPP)

Dispersed CGL was prepared by mixing DTPP pigment and polyvinylbutiral resin (PVB) binder (in a ratio of 3:1 by weight), dissolving in n-propanol (2% solid content), and dispersing them using a paint shaker. So that the dispersed mixture would contain electron acceptors, 0.2 mole of the electron acceptor material A9 was also added to 1 mole of the pigment. The resin mixture was then spin coated on an ITO substrate and dried at 100°C for an hour in a clean oven. The final thickness was 0.3 μm.

Formation of Charge Transfer Layer (CTL)

The CTL layer, which employed triphenylamine derivative (4Me-TPD) for the CTM, was made by mixing the CTM and polycarbonate resin (EUPIRON Z400: Mitsubishi Gas Chemicals, Japan) in a ratio of 3:1 by weight. The mixture was dissolved in the solvent consisting xylene spin coated on the substrate, and dried for two hours at 80°C in a clean oven. The amount applied was such that the final thickness was 10 μm after drying.

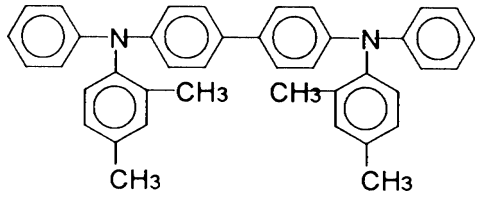

triphenylamine derivative (4Me-TPD)

Measurement of Photocurrent

A measuring cell was made by evaporating a 4 mm × 4 mm Au electrode on the CTL surface. The circuit shown in the previous article[5] was used to measure the photocurrent and dark current. A constant DC voltage was applied across the cell and monochromatic light with a wavelength of 560 nm from a monochromator illuminated the cell while the photocurrent was monitored on an oscilloscope. All measurements were made at room temperature.

Calculation of Quantum Yield

The photoinduced current is defined to be the current obtained by subtracting the dark current from the photocurrent. The quantum yield $\eta(t)$ is defined to be the ratio of the number of incident photons to the number of photogenerated electrons, estimated from the magnitude of the photoinduced current. The incident light had a wavelength of 560 nm and an intensity of 10 μW/cm² (2.82×10^{13} photons/cm²sec). The quantum yield is given by:

$$\eta(t) = \frac{6.24 \times 10^{18} \times \int_0^t I(t)dt}{2.82 \times 10^{13} \times t} \quad (1)$$

where t is the exposure time (sec), and $I(t)$ is the induced current (A/cm²).

Measurement of Resistivity

The resistivities of the CGL and PICAL were measured by the following method: After 500 Å-thick layers were formed on the surface of a glass substrate, a comb-shaped Au electrode formed on top by chemical vapor deposition; and standard current-voltage measurements were made. The resistivity is given by

$$\rho = \frac{l \cdot d}{w} \cdot \Delta \quad (2)$$

where w is the gap between the teeth of the comb electrode, l is the length of the electrode, d is the combined thickness of the CGL and PICAL, and Δ is the slope of

TABLE II. Photosensors with a PICAL

Type	PICAL
Reference	without a PICAL
Type-1	PVF resin, bis-azo pigment
Type-2	PVF resin, A9
Type-3	PVF resin, bis-azo pigment, A9

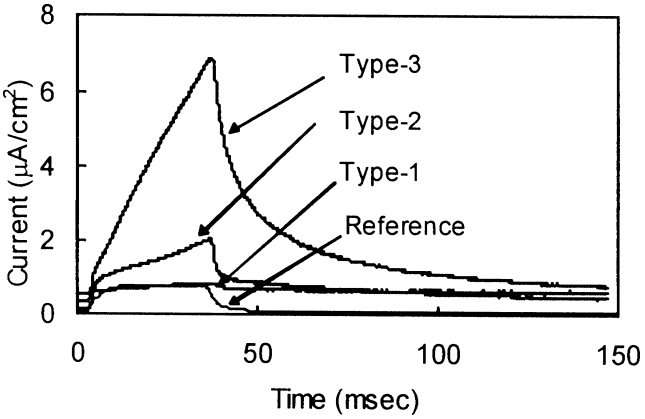

Figure 2. Photocurrent of the photosensors with various PICAL when light pulse was exposed. The light pulse was exposed to 560 nm, 3.0 μW/cm² for 33 msec. Applied voltage was 150 V DC.

the current-voltage curve (Δ = I/V). The actual values were: w = 0.2 mm, l = 37.5 mm, d = 500 Å.

Results and Discussion

Photocurrent Amplifying Effect of Three Layer Photosensor

The electrical characteristics of the Elgraphic photosensor depend on hole injection at the electrode/photoconductive layer interface, and electron trapping by electron acceptors seems to play a significant role in this region. In an attempt to control hole injection from the electrode, a layer containing electron acceptors was made between the electrode and the CGL, and the change in the photo and dark currents was examined. This layer is called the photoinduced current amplifying layer (PICAL).

A reference photosensor was fabricated by evaporating a CGL layer (thiopyrolopyrrole pigment: DTPP) on an ITO electrode, followed by a CTL layer. And following photosensors showed by Table II were fabricated by inserting a PICAL between the ITO electrode and CGL of the reference sensor. The amount of electron acceptor material added was 2% of the weight of PVF for Type-2, and 2% of the combined weight of CGM and PVF for Type-3. The thickness of the PICAL in all cases was 0.1 μm.

Figure 2 shows the transient photocurrent behavior of these sensors. These data were obtained by illuminating the sensors with 33 msec light pulses (560 nm, 3.0 μW) during the application of a 150V DC bias. While the two layer photosensor without a PICAL (Reference) showed blocking characteristics, the ones with a PICAL exhibited a photocurrent amplification capability. The Type-3 photosensor, which contained bis-azo pigment in addition to the electron acceptor material, showed more pronounced amplification.

The effect of the type of the electron acceptors (Table I) on the dark and photocurrents was examined. In all cases, the amount of electron acceptor materials added

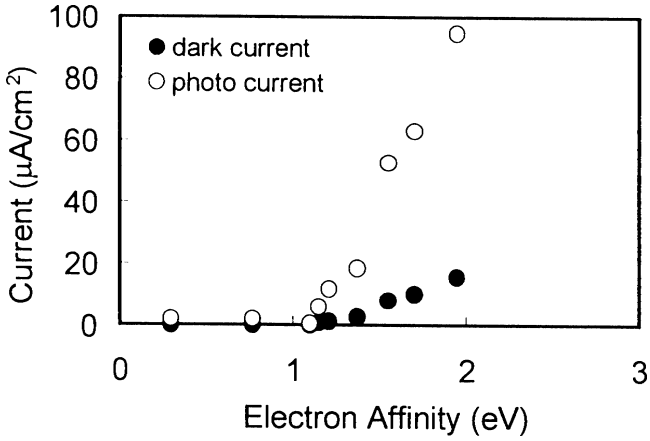

Figure 3. Photo and dark current of three layer photosensor over electron affinity of additive acceptor in PICAL. The light was exposed to 560 nm, 3.0 μW/cm². Applied voltage was 150 V DC.

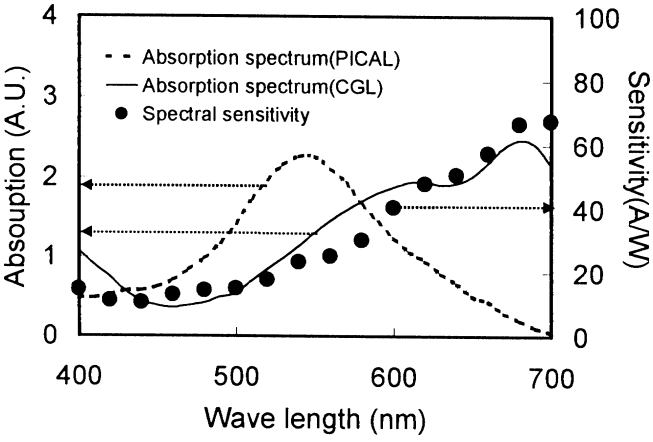

Figure 4. Spectral sensitivity of three layer photosensor and adsorption spectrum of PICAL and CGL.

was 8% of the combined weight of azo pigment and PVF. Figure 3 shows the photo and dark currents versus the electron affinity of the electron acceptor materials. All of the values shown in the figure are saturation values obtained under the application of a 150 V-DC bias and continuous exposure to monochromatic light (560 nm, 3.0 μW). The addition of an electron acceptor materials with an electron affinity greater than 1 eV to the PICAL proved effective in enhancing photocurrent amplification. These results agree with those for the two layer photosensors; electron traps deeper than 1 eV are needed to produce photoamplification.[5]

Spectral Sensitivity of Three layer Photosensor

Figure 4 shows a spectral sensitivity profile for a three layer photosensor, and absorption spectra of the CGL (DTPP pigment) and PICAL. It indicates that, in a three layer sensor, photocarriers are generated predominantly in the CGL.

Band Model of Photocurrent Amplifying Effect in Three Layer

Energy Diagram of a Three Layer Photosensor

Figure 5 shows an energy diagram of a three layer photosensor. The PICAL has three components: bis-azo

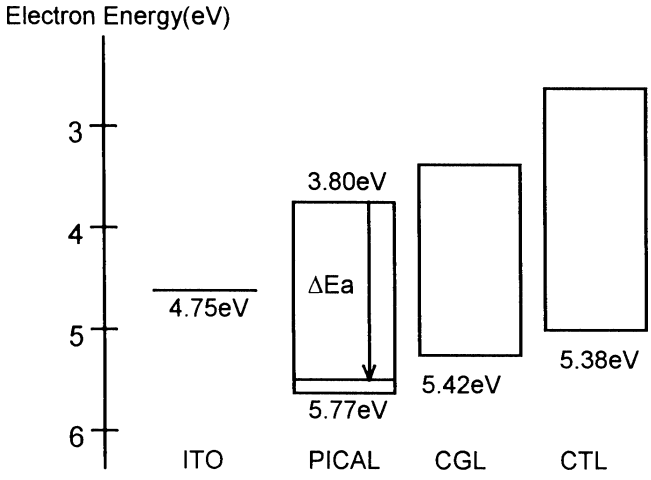

Figure 5. Energy diagram of three layer photosensor.

pigment, PVF resin, and the electron acceptor material A9. The ionization potential of the bis-azo pigment in the PICAL is 5.77 eV, and that of the DTPP pigment in the CGL is 5.42 eV. The difference between the ionization potentials suggests that the PICAL might raise the barrier to hole injection and stop the injection current from flowing. However, Fig. 2 clearly shows that it enhances both the dark current and photocurrent amplification more than a two layer sensor without a PICAL. This effect can be ascribed to the trapping of space charges by the electron acceptors, which lowers the barrier to hole injection.

Mechanism of Hole Injection

The photocurrent amplification mechanism in a three layer photosensor can be explained using the band diagram in Fig. 6. Figure 6(a) shows the initial accumulation of space charge after fabrication. The addition of bis-azo pigment to the PICAL increases the number of thermally excited carriers, and more electrons become trapped by the electron acceptors, thus lowering the barrier to hole injection. ($\Delta\phi_1$) Figure 6(b) shows that, when an electric field is applied, holes are injected from the electrode, resulting in the flow of dark current. In Fig. 6(c), photocarrier electrons generated in the CGL by illumination are injected into the PICAL and are trapped by the electron acceptors. Although photocarrier electrons generated in the PICAL can also be trapped by the electron acceptors, the CGL should absorb more light because it is much thicker than the PICAL. The net effect is a further lowering of the barrier to hole injection ($\Delta\phi_2$), enabling the flow of photoinduced current from the electrode.

Comparison of Photoamplification Characteristics: Two Layer versus Three layer Photosensors

Four types of photosensors were prepared (Fig. 7).

2L-EV-PS: A two layer sensor with a CGL formed by the chemical vapor deposition (CVD) of DTPP pigment on an ITO electrode.

2L-DP-PS: A two layer sensor with a CGL consisting of a dispersed mixture of DTPP pigment and PVB.

2L-DP+A9-PS: A two layer sensor that is a modification of 2L-DP-PS made by adding 0.2 mole of an electron acceptor material (A9) to one mole of the DTPP pigment.

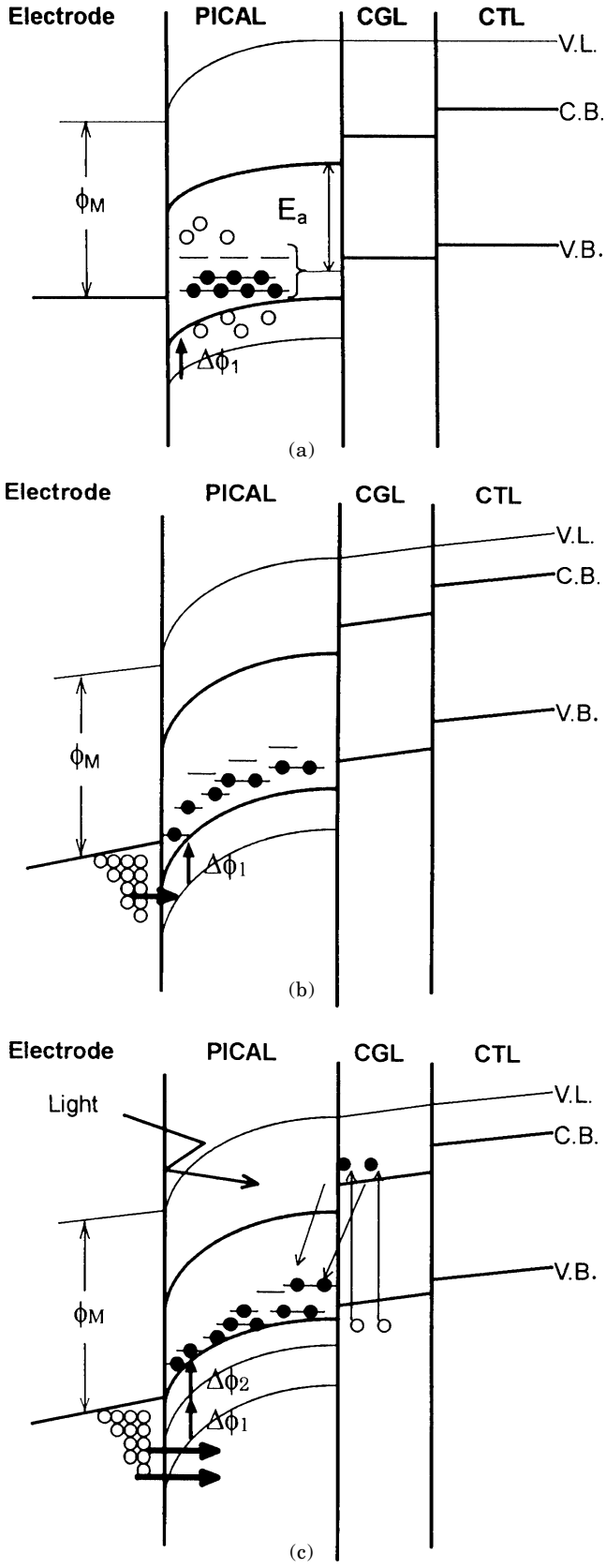

Figure 6. Band diagram of three layer photosensor without light exposure or applied voltage. (a) Thermal carriers are trapped in PICAL; (b) whole injection from electrode to three layer photosensor applied voltage only; (c) whole injection from electrode to three layer photosensor during light exposure with applied voltage. ○ hole, ● electron.

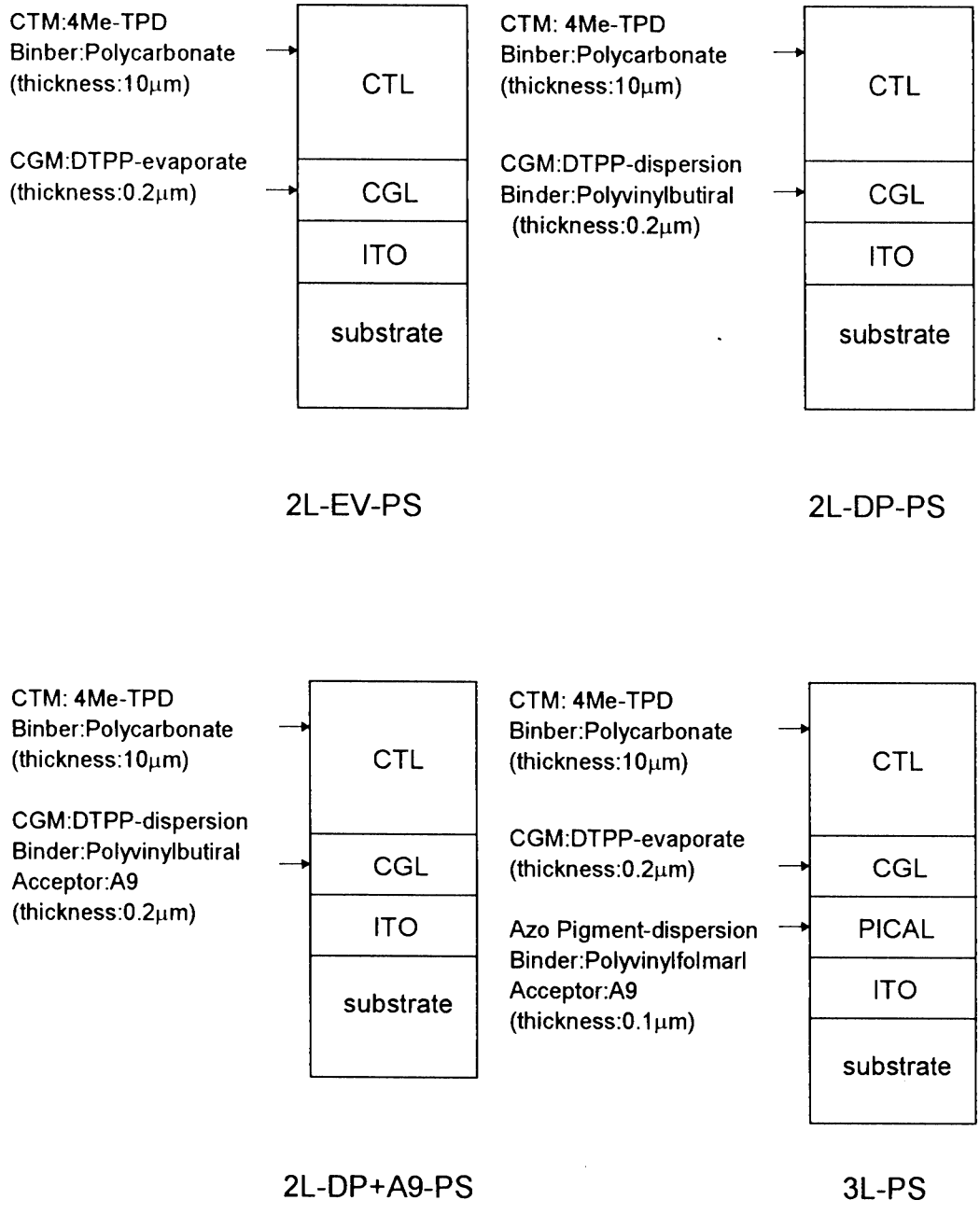

Figure 7. Structure of two and three layer sensors.

3L-PS: A three layer sensor based on 2L-EV-PS in which a third layer (PICAL) was formed between the ITO electrode and the CGL. The weight fraction of A9 in the PICAL was 8% of the combined weight of azo-pigment and PVF.

Figure 8(a) and 8(b) show the transient dark and photo current response of sensors exposed to monochromatic light pulses (560 nm, 10 μW/cm^2; pulse width = 33 msec) under a constant DC bias of 150 V. The light pulses struck the sensor 500 msec after the DC voltage was applied, by which time the system had reached the steady state.

As shown in Fig. 8(a), 2L-DP-PS and 2L-EV-PS both had very small dark currents (< 0.1 μA/cm^2). The behavior of the photocurrent was similar to that of the dark current, indicating that the photoconductivities of CVD and dispersed CGL layers are comparable. Figure 8(b) shows the behavior of the dark and photo currents of 3L–PS and 2L-DP+A9–PS. In these sensors the dark current became larger and the photocurrent increased during exposure (photocurrent amplification), which is attributable to the addition of the electron acceptor material A9. 3L–PS had a larger photoamplification current than 2L–DP+A9–PS. Figure 9 shows the time-wise change in the quantum yields of 2L–PS+A9 and 3L–PS. In both cases, the quantum yield exceeded unity,

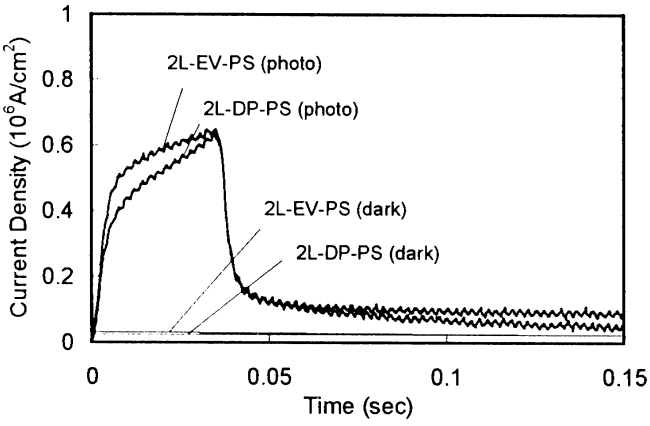

(a)

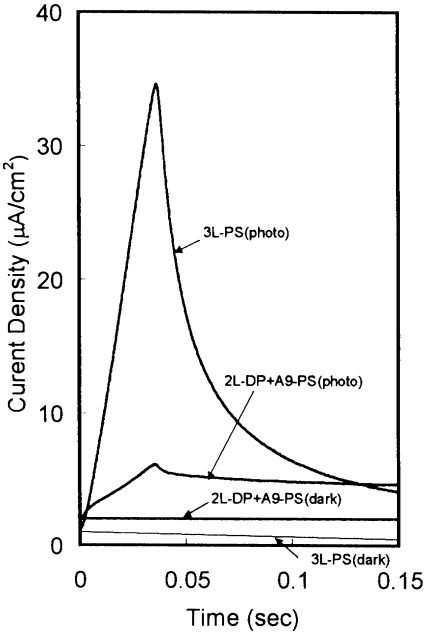

(b)

Figure 8. (a) Time-wise change in dark and photocurrents for 2L–EV-PS and 2L–DP–ES. Applied voltage: 150 V; illumination: Pulse (560 nm, 10 μW/cm^2) for 33 msec. (b) Time-wise change in dark and photocurrents for 2L–DP+A9–PS and 3L–PS. Applied voltage: 150 V; illumination: Pulse (560 nm, 10 μW/cm^2) for 33 msec.

indicating photocurrent amplification. The quantum yield of 3L–PS was larger than 40, which is significantly better than that of 2L–PS+A9.

In two layer Elgraphic photosensors, a larger dark current usually means greater photoamplification, assuming that the carrier production efficiency of the CGL is the same. In contradiction to this rule, 3L-PS had a larger photoinduced current than 2L-PS+A9, even though the former had a smaller dark current and the photoconductivities of dispersed and CVD films of DTPP pigment are comparable. It should also be noted that the dark current of 3L-PS showed a tendency to decrease 500 msec after the application of the DC bias and thereafter. These observations point to the existence of an additional photocurrent amplification mechanism inherent in the three layer structure, besides the mechanism related to the band model described above.

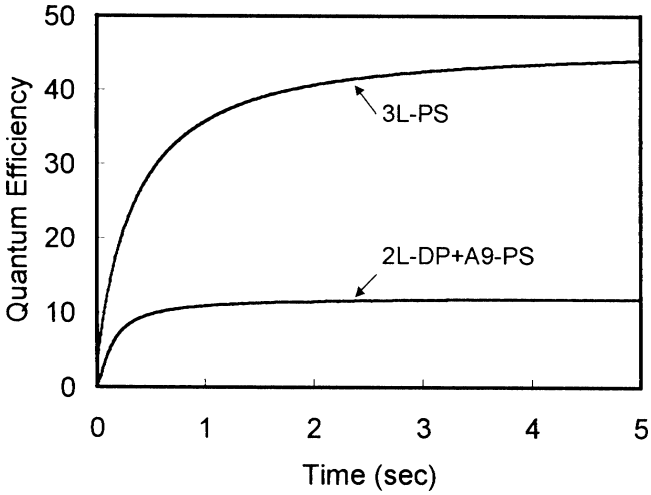

Figure 9. Time-wise change in quantum yield for 2L–DP+A9 and 3L–PS. Applied voltage: 150 V; illumination: Continuous (560 nm, 3.0 μW/cm^2).

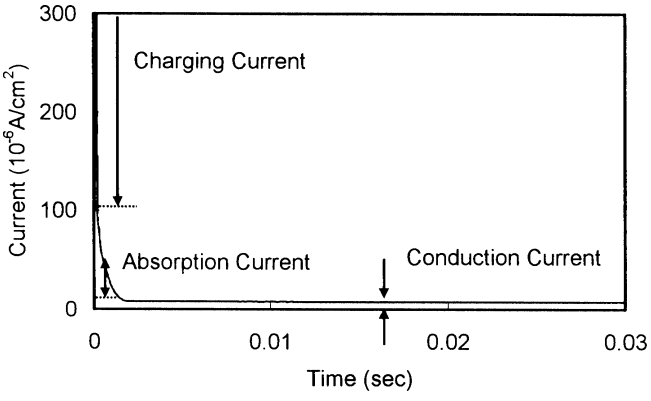

(a)

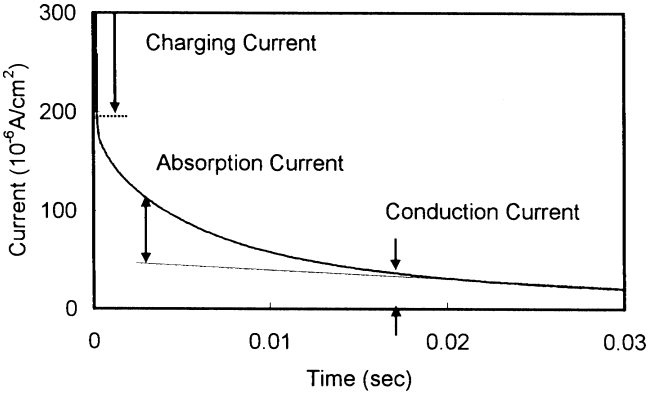

(b)

Figure 10. (a) Transient dark current immediately after application of CD voltage (Two layer sensor), applied voltage: 150 V; (b) Transient dark current immediately after application of CD voltage (Three layer sensor), applied voltage: 150 V.

Transient Response of Dark Current Immediately After Application of DC Voltage

Figure 10 shows the transient change in the dark current for two types of sensors that exhibit photocurrent amplification: 2L-DP+A9-PS and 3L-PS. The application

TABLE III. Resistivities of PICAL and CGL

Layer	Resistivity (Ω • cm)	
	Without exposure	With exposure
PICAL	1.18×10^7	1.21×10^7
CGL	1.62×10^7	3.64×10^6

of a DC voltage across a thin layer of organic dielectric generally induces charging, absorption, and conduction currents. In 2L-DP+A9-PS, after the charging current is flushed, the absorption current rapidly decreases and a constant conduction current persists [Fig. 10(a)]. In 3L-PS, a larger and more slowly decreasing absorption current appears after the charging current, and the conduction current also gradually decreases [Fig. 10(b)].

The absorption current density is assumed to be a function of the surface charge density of each dielectric layer. On that basis, when a DC bias is applied, the PICAL in 3L-PS probably has the effect of dynamically altering the voltage distribution across the CGL and PICAL, thus affecting hole injection from the electrode.

Resistivity of PICAL and CGL

500 Å-thick layers of a PICAL (with the fractional weight of A9 being 8% of the combined weight of azo-pigment and PVF) and a CGL (CVD DTPP pigment) were formed on a glass substrate, and a comb-shaped Au electrode was fabricated on it to make a measurement cell. The current-voltage characteristics were measured without exposure to light and under continuous exposure to monochromatic light (560 nm, 300 μW/cm²). The results are shown in Figs. 11(a) and (b); the relationships exhibit good linearity. The CGL with CVD DTPP pigment exhibits a decrease in resistance when exposed to light, indicating good photoconductivity. The PICAL, on the other hand, did not exhibit any photoconductivity when exposed to monochromatic light (300 μW/cm²) in the tested voltage region, even though it contained photoconductive azo-pigment. This phenomenon can be explained by the fact that azo-pigments require interaction with a CTM to exhibit photoconductivity, while DTPP pigment has this ability even in the absence of a CTM. The resistivities of the PICAL (ρ_{PICAL}) and CGL (ρ_{CGL}) were calculated from the slopes of the curves in Fig. 11 and are shown in Table III.

Without exposure to light, the resistivity of the PICAL is a bit smaller than that of the CGL ($\rho_{PICAL} < \rho_{CGL}$). Under exposure to monochromatic light with an intensity of 300 μW/cm², ρ_{PICAL} remains constant and ρ_{CGL} drops significantly, giving rise to an inversion of their relative magnitudes ($\rho_{PICAL} > \rho_{CGL}$). These data indicate that, in a three layer photosensor, an inversion of the relative magnitudes of ρ_{PICAL} and ρ_{CGL} occurs at a certain light intensity.

Equivalent Circuit Models of PICAL and CGL

The authors speculate that, in a three layer photosensor, the strength of the electric field across the PICAL, which was inserted between the electrode and the CGL, is the decisive factor in determining the amount of hole injection from the ITO electrode. Because the CTL is much thicker than the CGL or the PICAL, attention was focused on the strengths of the electric fields across the PICAL and the CGL. Figure 12 shows an equivalent circuit model consisting of a PICAL and CGL connected in

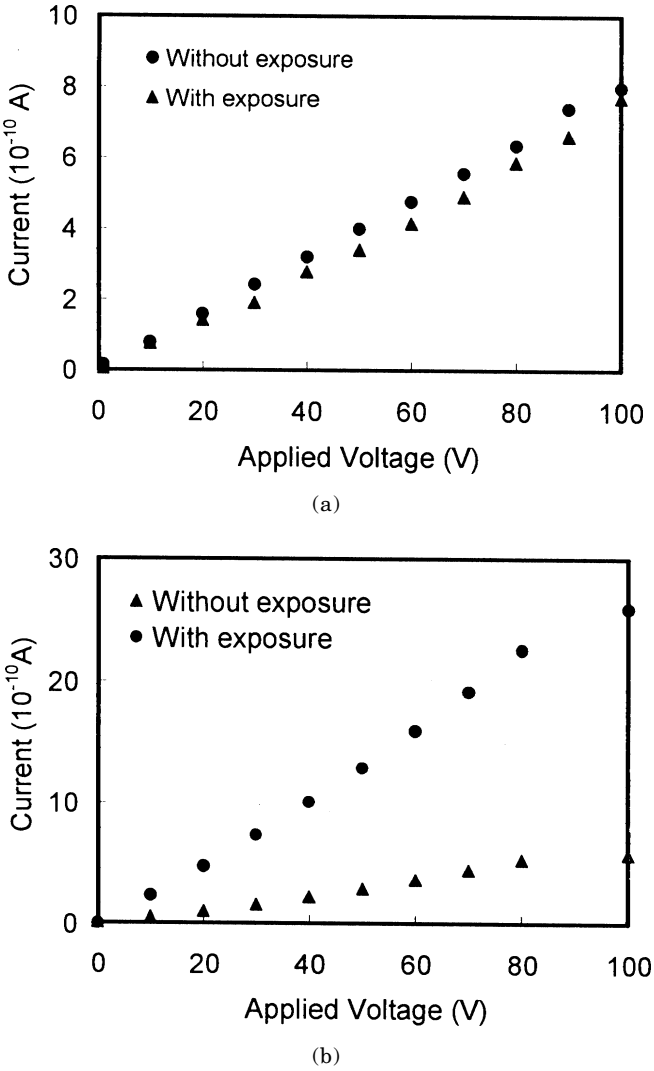

Figure 11. (a) I-V characteristics of PICAL. Light intensity: 300 μW/cm². (b) I-V characteristics of CGL. Light intensity: 300 μW/cm².

series, each of which is represented by a resister and a capacitor connected in parallel. In Fig. 12, ε_{CGL} and ε_{PICAL} are the relative dielectric constants, and d_{PICAL} (μm) and d_{CGL} (μm) is the thickness of the CGL and the PICAL, respectively. Letting S(m²) be the area of the sample, the resistances, R_{CGL} and R_{PICAL}, and the capacitances, C_{CGL} and C_{PICAL}, of the CGL and the PICAL can be calculated using the following expressions:

$$R_{CGL} = \rho_{CGL} \times \frac{d_{CGL}}{S} \tag{3}$$

$$R_{PICAL} = \rho_{PICAL} \times \frac{d_{PICAL}}{S} \tag{4}$$

$$C_{CGL} = 8.855 \times 10^{-12} \times \frac{\varepsilon_{CGL} S}{d_{CGL}} \tag{5}$$

$$C_{PICAL} = 8.855 \times 10^{-12} \times \frac{\varepsilon_{PICAL} S}{d_{PICAL}} \tag{6}$$

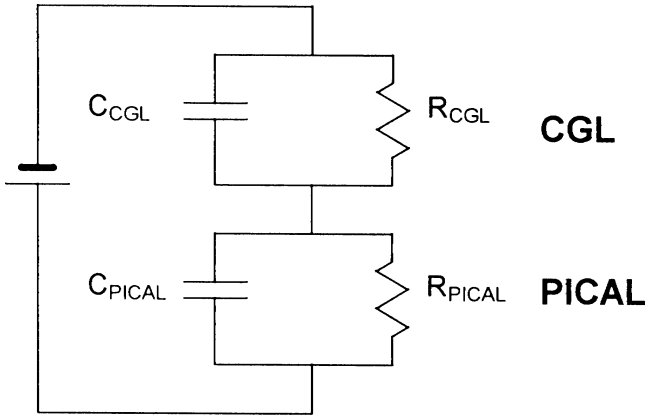

Figure 12. Equivalent circuit model of CGL and PICAL for three layer photosensor.

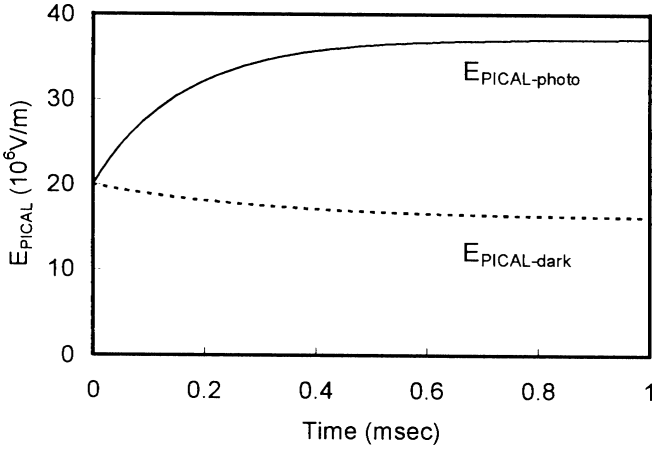

Figure 13. Time-wise change in strength of electric field across PICAL. Applied voltage for equivalent circuit in Fig. 9: 6 V. d_{PICAL} = 0.1 μm, d_{CGL} = 0.2 μm, $\rho_{\mathrm{PICAL}} = 1.18 \times 10^7$ Ωcm, $\rho_{\mathrm{CGL}} = 1.62 \times 10^7$ Ωcm (unexposed), $\rho_{\mathrm{CGL}} = 3.64 \times 10^6$ Ωm (exposed).

where the actual values are: $\varepsilon_{\mathrm{CGL}} = 2.7$, $\varepsilon_{\mathrm{PICAL}} = 2.4$, and $S = 1.6 \times 10^{-6}$ m^2.

Immediately after a voltage, V (volts), is applied, the voltage is divided between the CGL and the PICAL in inverse proportion to C_{CGL} and C_{PICAL}, respectively. As the system approaches the steady state, the voltage is divided in proportion to R_{CGL} and R_{PICAL}, respectively. The voltage across the PICAL at t seconds after it is applied is given by:

$$V_{PICAL}(t) = \frac{R_{PICAL}}{R_{CGL} + R_{PICAL}} + \left(\frac{C_{CGL}}{C_{CGL} + C_{PICAL}} V - \frac{R_{PICAL}}{R_{CGL} + R_{PICAL}} \right) e^{-\frac{t}{\tau}} \quad (7)$$

where

$$\tau = \frac{(C_{CGL} + C_{PICAL}) R_{CGL} R_{PICAL}}{R_{CGL} + R_{PICAL}} \quad (8)$$

The amount of electric charge flowing from one capacitor to another ($Q_{CAL}(t)$) is thought to correspond to the absorption current and is given by:

$$Q_{CAL}(t) = \frac{C_{CGL} R_{CGL} - C_{PICAL} R_{PICAL}}{R_{CGL} + R_{PICAL}} \left(1 - e^{-\frac{t}{\tau}} \right) V \quad (9)$$

Assuming that the thickness of the three layers in the photosensor is 0.1 μm for the PICAL, 0.2 μm for the CGL, and 10 μm for the CTL, and that the total voltage applied to the system is 150 V, then the voltage across the equivalent circuit for the series-connected CGL + PICAL is about 6 V. (The voltage is divided between the layers in inverse proportion to their capacitances). The change in the transient voltage across the PICAL (V_{PICAL}) was calculated, assuming the voltage across the CGL + PICAL to be 6 V, and using Eqs. 3 through 7 and also the values shown in Table I (Fig. 13). The vertical axis indicates electric field strength, $E_{PICAL} = V_{PICAL}/d_{PICAL}$, with $E_{PICAL-dark}$ being the value for unexposed areas and $E_{PICAL-photo}$ being for exposed areas. It is clear from Fig. 13 that, unlike $E_{PICAL-dark}$, which decreases over time, $E_{\mathrm{PICAL-photo}}$ increases over time until the system reaches the steady state, at which time $E_{PICAL-photo}$ is more than twice as large as $E_{PICAL-dark}$. In a two layer photosensor without a PICAL, the model does not predict this type of transient behavior; the electric field strength is the same for both exposed and unexposed areas (20×10^6 V/m). If the assumption that the voltage across the PICAL has the effect of enhancing hole injection from the electrode is correct, then the additional layer in a three layer photosensor increases the injection current in areas exposed to light, thus increasing the apparent quantum yield in those areas.

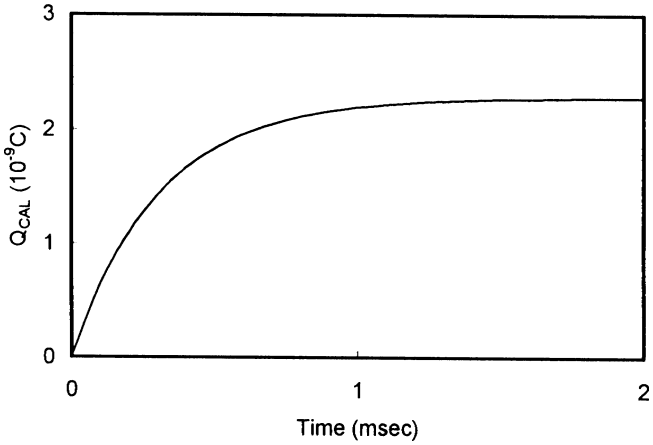

Figure 14. Electric charge flowing through CGL and PICAL over time. Applied voltage for equivalent circuit in Fig. 9: 6 V. d_{PICAL} = 0.1 μm, d_{CGL} = 0.2 μm, $\rho_{\mathrm{PICAL}} = 1.18 \times 10^7$ Ωcm, $\rho_{\mathrm{CGL}} = 1.62 \times 10^7$ Ωcm (unexposed), $\rho_{\mathrm{CGL}} = 3.64 \times 10^6$ Ωcm (exposed).

Figure 14 shows the transient current that flows between the two capacitors ($Q_{CAL}(t)$) for no exposure, as calculated from Eqs. 3 through 6 and Eq. 8. The calculated total charge is about 2.2 nC. The charge (Q_{exp}) obtained from integrating the absorption current over time in Fig. 6(a) is about 3.9 nC. Based on these results, the authors believe the equivalent circuit model to be a fairly accurate representation of an actual sensor.

Conclusion

Three layer photosensors, which have a photoinduced current amplifying layer (PICAL) between the ITO electrode and CGL, were fabricated and their photocurrent amplification capability was investigated. The PICAL contained a certain amount of electron acceptor material.

Just as for two layer sensors, the photoamplification can be attributed to the lowering of the hole injection barrier due to electrons trapped at the electrode interface. However, three layer sensors exhibited better characteristics, namely, a smaller dark current and a larger photoinduced current. It results from that the strength of the electric field across the PICAL is larger in areas exposed to light and smaller in unexposed areas.

It was concluded that in three layer sensors there are two distinct mechanisms; one involving the trapping of a space charge at the electrode/photoconductive layer interface, and the other involving the difference in resistivity between the two bulk layers (CGL and PICAL). These mechanisms work together to produce stronger photocurrent amplification than that occurring in two layer sensors.

Acknowledgment. The authors would like to thank Mr. Yasuo Yamaji and Kuniaki Kamei for their encouragement and support throughout this study.

References

1. M. Utsumi, M. Akada, and E. Inoue, in *Proc. IS&T's 48th Annual Conference*, IS&T, Springfield VA, 1995, p. 499.
2. M. Akada, D. Aoki, H. Kamiyama, and E. Inoue, in *Proc. IS&T's 49th Annual Conference*, IS&T, Springfield VA, 1996, p. 290.
3. H. Kamiyama, M. Utsumi, H. Hikosaka, M.Akada, T. Toida, and E. Inoue, *J. Imaging Sci. Technol.* In press.
4. D. Aoki, S. Sakano, M. Okabe, O. Shimizu, M. Utsumi, M. Akada, and E. Inoue, in *Proc. IS&T's 48th Annual Conference*, IS&T, Springfield VA, 1995, p. 502.
5. D. Aoki, M. Okabe, S. Hikosaka, and E. Inoue, *J. Imaging Sci. Technol.* **44**(2): 120 (2000).